JACS
JOURNAL OF THE AMERICAN CHEMICAL SOCIETY
Article
pubs.acs.org/JACS

Optimized Phospholipid Bilayer Nanodiscs Facilitate High-Resolution Structure Determination of Membrane Proteins

Franz Hagn, Manuel Etzkorn,‡ Thomas Raschle,‡ and Gerhard Wagner*

Department of Biological Chemistry and Molecular Pharmacology, Harvard Medical School, 240 Longwood Avenue, Boston, Massachusetts 02115, United States

Supporting Information

ABSTRACT: Structural studies of membrane proteins are still hampered by difficulties of finding appropriate membrane-mimicking media that maintain protein structure and function. Phospholipid nanodiscs seem promising to overcome the intrinsic problems of detergent-containing environments. While nanodiscs can offer a near-native environment, the large particle size complicates their routine use in the structural analysis of membrane proteins by solution NMR. Here, we introduce nanodiscs assembled from shorter ApoA-I protein variants that are of markedly smaller diameter and show that the resulting discs provide critical improvements for the structure determination of membrane proteins by NMR. Using the bacterial outer-membrane protein OmpX as an example, we demonstrate that the combination of small nanodisc size, high deuteration levels of protein and lipids, and the use of advanced non-uniform NMR sampling methods enable the NMR resonance assignment as well as the high-resolution structure determination of polytopic membrane proteins in a detergent-free, near-native lipid bilayer setting. By applying this method to bacteriorhodopsin, we show that our smaller nanodiscs can also be beneficial for the structural characterization of the important class of seven-transmembrane helical proteins. Our set of engineered nanodiscs of subsequently smaller diameters can be used to screen for optimal NMR spectral quality for small to medium-sized membrane proteins while still providing a functional environment. In addition to their key improvements for *de novo* structure determination, due to their smaller size these nanodiscs enable the investigation of interactions between membrane proteins and their (soluble) partner proteins, unbiased by the presence of detergents that might disrupt biologically relevant interactions.

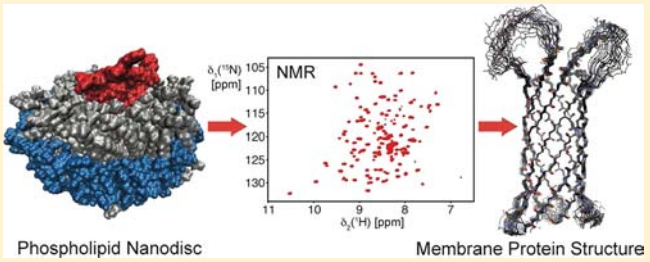

INTRODUCTION

Compared to the plethora of structural data on soluble proteins, much less is known about structures of integral membrane proteins. This is primarily due to difficulties of producing integral membrane proteins in folded and active forms as well as in sufficient yields. A major part of this problem is the selection of an appropriate membrane-mimicking environment supporting both function and stability of a particular membrane protein. Usually detergents are employed for membrane protein preparation, and detergent micelles are the most common media for structural investigations.[1] However, crystal structures of membrane proteins solubilized in detergents often contain bound lipids, emphasizing the beneficial effect of a lipid environment for their structure and stability.[2] Detergents may also lower membrane protein stability and abolish their biological function.[3] In addition, detergents can hamper interaction studies between membrane proteins and soluble factors, as they tend to destabilize or even denature soluble interaction partners. The use of phospholipid bilayers can overcome these problems, as they resemble a considerably more native membrane environment. Phospholipid bilayers can be prepared to match any desired lipid composition, required to stabilize the respective membrane protein. Until recently, phospholipid liposomes were the only means to harbor membrane proteins in a detergent-free bilayer environment. Unfortunately, liposomes are not compatible with crystallization, and these particles are too big for solution-state NMR as well. Among NMR methods, solid-state NMR has made progress in studying membrane proteins in large phospholipid bilayer systems,[6] but signal overlap and low sensitivity are often preventing structural work at high-resolution.

The recent introduction of phospholipid nanodiscs as membrane mimetic[5,7,8] appears promising for studying membrane proteins in phospholipid bilayers by solution NMR. The formation of nanodiscs is based on the observation that apolipoprotein A-I (ApoA-I) can wrap around small patches of bilayers, creating small, membrane-like particles of defined size.[9,10] Different versions of Apo A-I have been engineered for biophysical studies and are called membrane scaffold proteins (MSPs).[5] Ideally, two copies of MSPs wrap around a patch of a lipid bilayer to form a disc-like particle or nanodisc (Figure 1A). This system has the potential to be a

Received: November 9, 2012
Published: January 8, 2013

   dx.doi.org/10.1021/ja310901f | J. Am. Chem. Soc. 2013, 135, 1919−1925

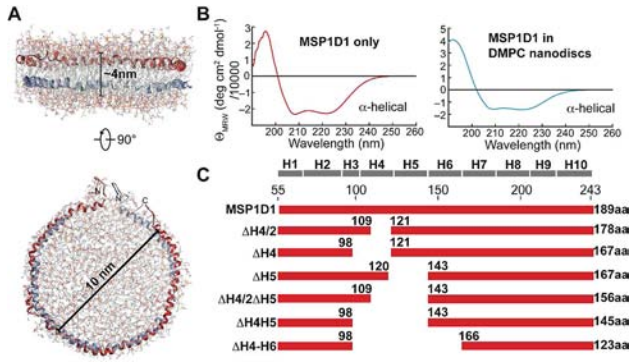

Figure 1. Construction of truncated membrane scaffold protein (MSP) variants. (A) Proposed architecture of a phospholipid nanodisc where two copies of MSPs wrap around a patch of phospholipid bilayer, thereby stabilizing its hydrophobic edge. The most commonly used nanodisc has a diameter of 10 nm. Coordinates of the MSP were taken from ref 4. (B) Far-UV CD spectra of MSP alone (left) or in an assembled nanodisc (right) show that MSP adopts α-helical secondary structure in both cases. (C) Deletion constructs of MSP1D1[5] used in this study. The predicted secondary structure of MSP1D1 is shown on top, and the length of each construct is indicated.

widely used membrane mimetic with the advantage of closely resembling a native-like lipid environment.[5] To this end, nanodiscs are the only available detergent-free membrane mimetic for solution NMR spectroscopy that are suitable for studying protein−protein interactions in an unbiased lipid bilayer environment. It is therefore highly desirable to be able to structurally characterize membrane proteins in this promising system by NMR. The shortest commonly used version of the MSP constructs produces discs of around 10 nm in diameter, which translates into a molecular weight of 150−200 kDa. These nanodiscs were already successfully used for the incorporation of membrane proteins like VDAC-1[11] and VDAC-2,[12] CD4mut,[13] and the voltage-sensing domain of the potassium channel KvAP[14] for 2D heteronuclear NMR experiments. However, the use of nanodiscs for multidimensional NMR experiments as required for structure determination remained elusive due to the still large molecular weight of these particles.

Here, we present a set of truncated ApoA-I variants that form smaller nanodiscs suitable for NMR studies of small to medium-sized membrane proteins. We were able to reduce the nanodisc diameter by up to 3.0 nm from the 10 nm obtained with wild-type MSP1D1[5] protein construct, as estimated by size exclusion chromatography (SEC), dynamic light scattering (DLS), and electron microscopy (EM). To assess the NMR spectroscopic properties, we incorporated the bacterial outer membrane β-barrel protein OmpX and the seven-transmembrane α-helical protein bacteriorhodopsin into this set of nanodiscs. We evaluated the spectral quality by 2D-[^{15}N;^{1}H]-TROSY and TROSY for rotational correlation times (TRACT) experiments and used circular dichroism (CD) spectroscopy to assess the thermal stability of OmpX in each nanodisc. Furthermore, we show that OmpX incorporated into smaller nanodiscs is accessible to multidimensional NMR experiments, enabling resonance assignment and high-resolution structure determination. The obtained structure of OmpX in phospholipid nanodiscs was compared to the structure in dodecylphosphocholine (DPC) detergent micelles determined here, as well as to the previously reported NMR structure in dihexanoyl-glycero-phosphocholine (DHPC) detergent micelles[15] and to the crystal structure in *n*-octyltetraoxyethylene (C_8E_4).[16] Finally, we characterized the dynamics of the obtained structures in phospholipid nanodiscs and DPC micelles using NMR relaxation experiments and molecular dynamics (MD) simulations.

RESULTS

Construction of Truncated Membrane Scaffold Protein Variants. The most commonly used nanodisc has a diameter of around 10 nm and a molecular weight of 150−200 kDa (Figure 1A). In order to construct a truncated set of MSPs, we assumed that the size of a nanodisc particle is solely governed by the length of the MSP.[7] To get a raw estimate on the correlation between MSP length and nanodisc size, we analyzed the apolipoprotein A-I crystal structure (PDB code: 1av1[17]).

The protein consists of a single α-helix interrupted by kinks caused by proline residues. The α-helical secondary structure content of this protein in solution was confirmed by CD spectroscopy (Figure 1B). Taking into account the number of amino acids of MSP1D1 (189aa) and assuming an α-helical pitch per residue of 0.15 nm, a theoretical length of 28.5 nm can be derived, resulting in a diameter of 9.1 nm. The thickness of the helical MSP contributes approximately 0.5 nm to the diameter on each side of the disc, resulting in a total diameter of about 10 nm, which is close to the value of 9.6 nm determined experimentally.[5] We also modeled the dimensions of the nanodisc formed by MSP1D1 using the empirically determined number of 80 dimyristoylphosphatidylcholine (DMPC) lipid molecules per bilayer leaflet, which resulted in a diameter of 8 nm for the lipid bilayer alone. Adding 1 nm for the diameter of the MSP protein at each side of the nanodisc results in a final diameter of 10 nm, which is in excellent agreement with the experimentally determined size.[5] It seems generally possible to predict the size of the assembled nanodiscs on the basis of either the length of the MSP protein or the number of lipids per MSP.

In order to design smaller nanodiscs, we focused on the deletion of internal regions of the MSP, resulting in the construction of a series of MSPs lacking either (half of) helix 4, helix 5, helix 4 and 5, or helix 4−6 (Figure 1C). Deletion of N-terminal residues of MSP1D1 produced only slightly smaller nanodiscs (Figure S1), which is in agreement with previous observations.[5] However, DMPC nanodiscs formed with the internally shortened MSPs showed markedly altered lipid-to-MSP ratios and elution profiles in analytical SEC experiments (Figure 2A), yielding nanodiscs of subsequently smaller sizes (Figure 2B). Using different MSP-to-lipid (DMPC) ratios (Table 1), we empirically optimized the number of lipid molecules per nanodisc. The smallest disc (MSP1ΔH4−H6) harbors only 10 DMPC molecules per MSP protein, which corresponds to an area of roughly 500 Å^2 per bilayer leaflet. The size of this series of nanodiscs was further estimated by DLS and EM (Table 1, Figure 2C, Figure S2). In line with the SEC data, a decrease in nanodisc diameter by as much as ~3 nm could be detected from the initial MSP1D1 construct using EM and DLS. In good agreement with the experimental data, modeling of a bilayer based on the known number of lipids in each disc predicts their size fairly well (Figure 2D, Table 1). We furthermore validated the long-term stability of the smaller discs by recording SEC experiments 50 days after nanodisc assembly. As evident by the gel filtration elution profiles (Figure S2), the smallest nanodisc presented here (with

dx.doi.org/10.1021/ja310901f | J. Am. Chem. Soc. 2013, 135, 1919−1925

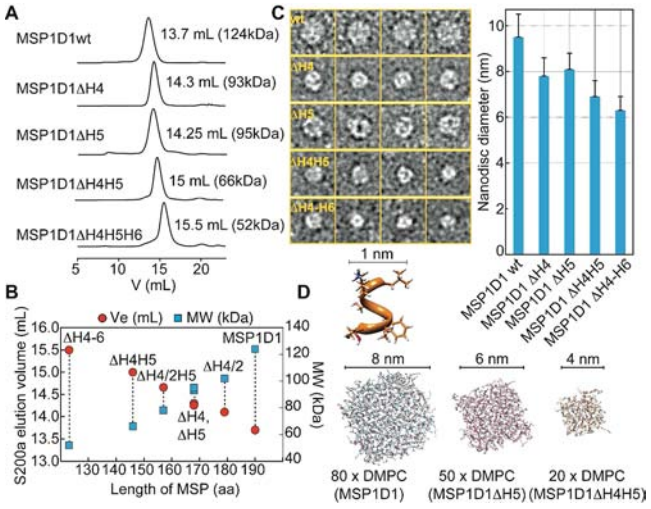

Figure 2. Characterization of the smaller nanodiscs. (A) Size exclusion chromatograms of DMPC nanodiscs formed with various MSP1 deletion variants as indicated. The molecular weight was obtained by calibration of an analytical S200 column. (B) The elution volumes and the calculated molecular weights are linearly dependent on the length of the MSP protein that is in contact with lipids. (C) Representative negative-stain electron micrograms showing single nanodisc particles for the MSP variants as indicated. Right: Average diameter of nanodisc preparations determined by single particle analysis showing a decrease in nanodisc diameter from 9.5 to 6.3 nm with shorter MSP variants. Error bars indicate standard deviations (see also Figure S2). (D) Assembly and equilibration of the experimentally determined number of DMPC lipids for MSP1D1, MSP1D1ΔH5 and MSP1D1ΔH4H5 by MD simulations provide a fairly good estimate of the diameter of each nanodisc. To obtain the final diameter, one layer of the helical MSP protein (1 nm) was added to each side of the lipid bilayer.

MSP1D1ΔH4–6) shows a tendency to form larger assemblies of approximately 11 nm diameter over time; a similar behavior was previously observed for Apolipophorin-III lipoprotein particles.[18] To a lower extent, this feature can also be observed for the MSP1D1ΔH4H5 nanodisc, whereas the other discs presented here are stable over the investigated time period (Figure S2).

Application to Seven-Transmembrane Helical Protein Bacteriorhodopsin. In order to test the smaller discs for the use in NMR spectroscopy, we first used the seven-transmembrane helical protein bacteriorhodopsin (bR). bR is a well-characterized membrane protein that can be produced in rather good amounts by *Escherichia coli* cell-free expression techniques[19] (see SI methods). Analytical SEC indicates that bR can be incorporated into our smaller discs (Figure 3A). The

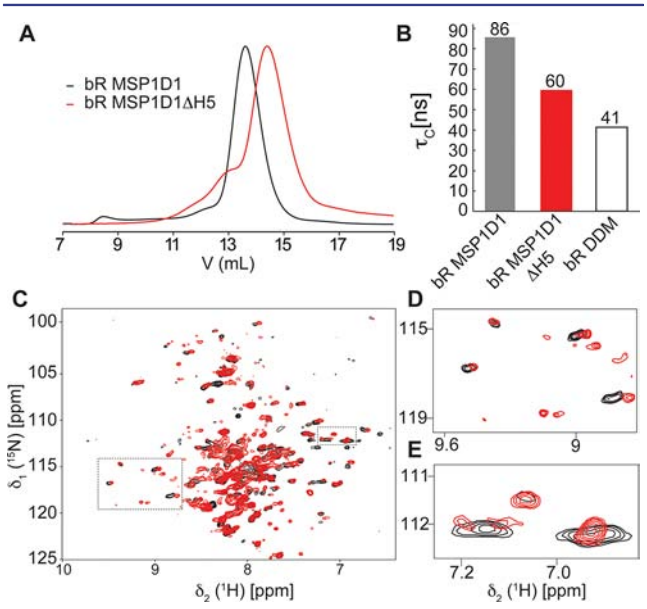

Figure 3. Analysis of bacteriorhodopsin (bR) in different nanodiscs. (A) Analytical SEC traces of bR assembled into nanodiscs of different sizes. (B) Apparent rotational correlation time (τ_c) of bR in DMPC MSP1D1 (black) and MSP1D1ΔH5 (red) nanodiscs and in DDM micelles (white). (C) Overlay of ^{15}N–^{1}H-TROSY spectra of bR in MSP1D1 (black) and MSP1D1ΔH5 (red). (D,E) Expansion of boxed regions in (C).

functionality and the presence of an intact tertiary structure of the preparation were further corroborated by its characteristic purple color. The apparent correlation time of ^{2}H- and ^{15}N-labeled bR in MSP1D1ΔH5 and MSP1D1wt DMPC nanodiscs and *n*-dodecyl *β*-D-maltopyranoside (DDM) micelles was estimated with [^{15}N,^{1}H]-TRACT experiments[20] (Figure 3B). A pronounced reduction (>20 ns) in the apparent correlation time of bR can be seen with the ΔH5 variant as compared with wild-type MSP. However, bR in DDM micelles shows an even smaller correlation time. These results are in line with reduced proton line widths of the ^{1}H–^{15}N correlation signals in a 2D-TROSY experiment (Figure 3D,E, Figure S3). Our data hence suggest that the optimized discs have the potential of significantly improving the spectral quality of seven-transmembrane helical proteins when compared to the nanodisc

Table 1. Size and Lipid Content of Nanodiscs Used in This Study

MSP protein	MSP:DMPC ratio	SEC V_e, MW, $2R_h$[a]	EM diameter	NMR τ_c,[b] calcd MW	DLS[c] $2R_h$, MW	calcd[d] diameter
MSP1D1wt	1:80	13.7 mL, 124 kDa, 10.2 nm	9.5 ± 1.1 nm	48 ns, 158 kDa	9.4 ± 0.9 nm, 126 kDa	9.5 nm
ΔH4/2	1:60	14.10 mL, 102 kDa, 9.4 nm	n.d.	n.d.	n.d.	8.9 nm
ΔH4	1:45	14.3 mL, 93 kDa, 9.1 nm	7.8 ± 0.8 nm	33 ns, 102 kDa	8.2 ± 0.9 nm, 91 kDa	8.2 nm
ΔH5	1:50	14.25 mL, 95 kDa, 9.2 nm	8.2 ± 0.6 nm	34 ns, 107 kDa	8.4 ± 0.7 nm, 98 kDa	8.4 nm
ΔH4/2H5	1:30	14.66 mL, 78 kDa, 8.4 nm	n.d.	n.d.	n.d.	7.9 nm
ΔH4H5	1:20	15 mL, 66 kDa, 7.8 nm	6.9 ± 0.8 nm	27 ns, 81 kDa	7.3 ± 0.3 nm, 70 kDa	7.1 nm
ΔH4-H6	1:∼10	15.5 mL, 52 kDa, 6.8 nm	6.3 ± 0.6 nm (10.9 ± 0.9 nm)	n.d.	6.4 ± 0.5 nm, 52 kDa	6.3 nm

[a] R_h = hydrodynamics radius. [b] τ_c = rotational correlation time, obtained with [^{15}N,^{1}H]-TRACT experiments at 318K with ^{2}H,^{15}N-labeled OmpX. [c] DLS = dynamic light scattering. [d] Calculated using the formula $D = (n(\text{aa}) \times 0.15\ \text{nm}/\pi) + 1\ \text{nm}$, where n(aa) is the number of amino acids in contact with lipids, which is 180 for MSP1D1.

dx.doi.org/10.1021/ja310901f | J. Am. Chem. Soc. 2013, 135, 1919–1925

constructs reported so far, promoting their use for the NMR investigation of proteins with similar topology.

Even though NMR spectral quality of bR is better in detergent micelles, the higher stability in phospholipid nanodiscs may still be beneficial for performing long-term experiments and interaction studies. This may be even more critical for less stable proteins with a comparable membrane topology.

Strategy for Screening Optimal Nanodisc Size for OmpX. We next chose the bacterial outer membrane protein OmpX for incorporation into phospholipid nanodiscs. The smaller size of this membrane protein (148aa) is expected to allow the use of a wide range of nanodisc variants. We compared DMPC/dimyristoylphosphatidylglycine (DMPG) (3:1) nanodiscs made with MSP1D1wt and the ΔH5 and ΔH4H5 variants by recording 2D-[^{15}N,^{1}H]-TROSY and TRACT experiments. A cartoon of the resulting OmpX nanodiscs is depicted in Figure 4A, showing OmpX and the

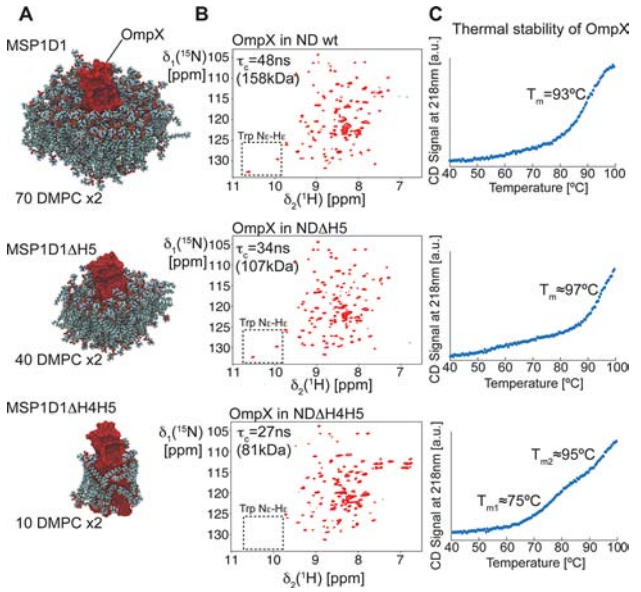

Figure 4. Optimization of nanodisc size for the target protein OmpX. (A) Equilibrated box with OmpX and the number of DMPC lipids per bilayer leaflet determined experimentally. For clarity, the surrounding MSP protein is not shown. (B) 2D-[^{15}N,^{1}H]-TROSY experiments with ^{2}H,^{15}N-labeled OmpX in nanodiscs of different sizes, as indicated in the figure. The spectral region of the tryptophan side-chain resonances is marked with a box. (C) Circular dichroism (CD)-detected thermal unfolding traces at 218 nm of OmpX in different nanodiscs.

determined number of lipids in each preparation. The nanodisc made from MSP1D1ΔH4H5 accommodates approximately 10 lipid molecules per bilayer leaflet in addition to OmpX, thus barely forming a one-layered ring of lipids around the protein. 2D-[^{15}N,^{1}H]-TROSY spectra of each preparation is shown in Figure 4B. Compared to the wild-type nanodisc, the spectral quality of the OmpX 2D-[^{15}N,^{1}H]-TROSY improves with the MSP1D1ΔH5 nanodisc. Due to the low amount of lipid present in the smallest discs (MSP1D1ΔH4H5), the side-chain resonances of the two tryptophan residues (boxes in Figure 4B) disappear, most likely due to altered dynamics or enhanced relaxation caused by direct contact between OmpX and the MSP protein. The rotational correlation times estimated with TRACT experiments (Figure S4) indicate smaller particle sizes with shorter MSP variants (τc and MW statements in Figure 4B). However, CD-detected thermal melting curves show that only MSP1D1wt and ΔH5 represent a stable environment for OmpX, whereas the melting transition of the ΔH4H5 nanodisc at around 75 °C indicates lower stability. A comparison of proton relaxation rates of lipid resonances in wild-type and ΔH5 nanodiscs suggests similar lipid dynamics in both systems, indicating that the relative restrictions imposed on the phospholipids in the bilayer by the smaller scaffold protein are very similar (Figure S5). In summary, the MSP1D1ΔH5 nanodisc of an apparent molecular weight of 107 kDa was best suited for further NMR studies of OmpX and was therefore selected for all subsequent experiments. The CD-detected high thermal stability of this nanodisc preparation permits NMR experiments at elevated temperatures.

NMR Resonance Assignment and Structure Determination of OmpX in Phospholipid Bilayer Nanodiscs. For 3D backbone resonance assignment experiments, we used uniformly ^{2}H,^{13}C,^{15}N-labeled OmpX in MSP1D1ΔH5 nanodiscs assembled with deuterated DMPC/DMPG (3:1) lipids. A set of TROSY 3D triple-resonance experiments consisting of HNCO, HN(CA)CO, HNCA, HN(CO)CA, and HN(CA)CB[22] was recorded in a non-uniformly sampled (NUS) manner at 45 °C. The sampling schedules for all 3D experiments were generated using the Poisson−Gap method,[23] and the final spectra were reconstructed by the iterative soft threshold method.[24] This procedure produced sharp line widths and enabled the detection of most of the expected resonances in each of the NMR experiments. In contrast to the smaller nanodiscs, HNCACB-type experiments were not successful with MSP1D1 nanodiscs due to their large size leading to enhanced transverse relaxation, which prevented the desired coherence transfer. The good quality and high resolution of the 3D NMR experiments (Figure 5A,B) in smaller nanodiscs facilitated the resonance assignment of 90% of all non-proline residues. Some residues in loop regions and around Trp140 and Ser130 could not be assigned, most likely due to unfavorable dynamics and fast amide hydrogen exchange at 45 °C. The extracted chemical shift data were used to identify the eight β-strands in the protein (Figure 5C). Furthermore, a ^{15}N-edited 3D-TROSY-NOESY experiment was used to detect long-range inter-β-strand contacts (Figure 6A) that enabled the structure determination of OmpX in nanodiscs. The degree of assignment and the location of the interstrand NOE contacts are graphically summarized in Figure 6B. In order to compare the structure of OmpX in a nanodisc and a micellar environment, we additionally performed NMR backbone assignment and NOESY experiments with OmpX in DPC micelles (Figures S6 and S7).

A similar degree of backbone resonances and NOE contacts could be assigned (Table 2). Chemical shift data, NOE distance, and hydrogen bond restraints were subsequently used to determine the structure of OmpX in both membrane mimics (Table 2). The ensemble of the 20 lowest-energy models of OmpX in phospholipid nanodiscs (Figure 6C) shows a root-mean-squared deviation (rmsd) of 0.32 Å for ordered secondary structural elements. In both environments the residues in the extracellular loops 3 and 5 show no long-range NOEs, exhibit rapid amide-hydrogen exchange, and in contrast to the crystal structure of OmpX[16] do not adopt a rigid β-sheet conformation. The chemical shift values of OmpX in both environments are very similar except for the long loop regions and, to a smaller extent, in some of the β-stands (Figure

dx.doi.org/10.1021/ja310901f | J. Am. Chem. Soc. 2013, 135, 1919−1925

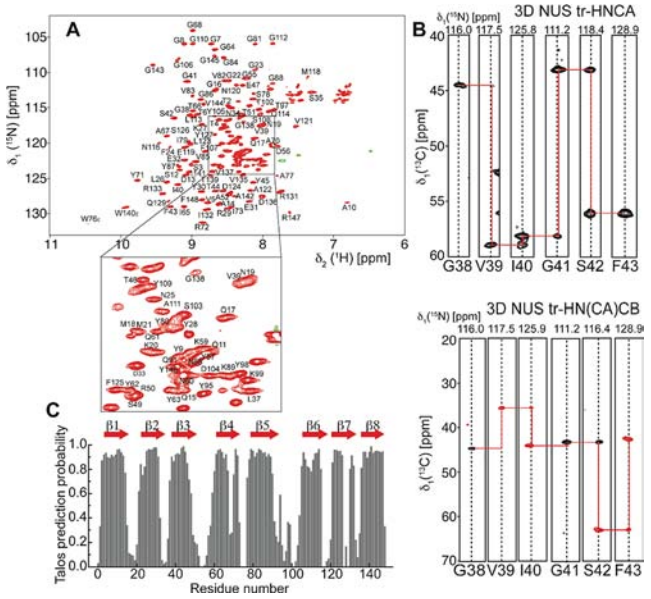

Figure 5. NMR backbone assignment and secondary structure determination of OmpX in MSP1D1ΔH5 nanodiscs. (A) 2D-[^{15}N,^{1}H]-TROSY spectrum of OmpX in MSP1D1ΔH5 DMPC/DPMG (3:1) nanodiscs at 45 °C and pH 6.8. All assigned non-proline backbone amide resonances (90%) are labeled in the spectrum. (B) Example strips taken from the 3D-NUS HNCA and HN(CA)CB experiments show high spectral quality and resolution required for backbone resonance assignment. (C) Secondary structure prediction taken from the program Talos+ [21] indicates eight β-strands and long loop regions between strands 3 and 4 and strands 5 and 6.

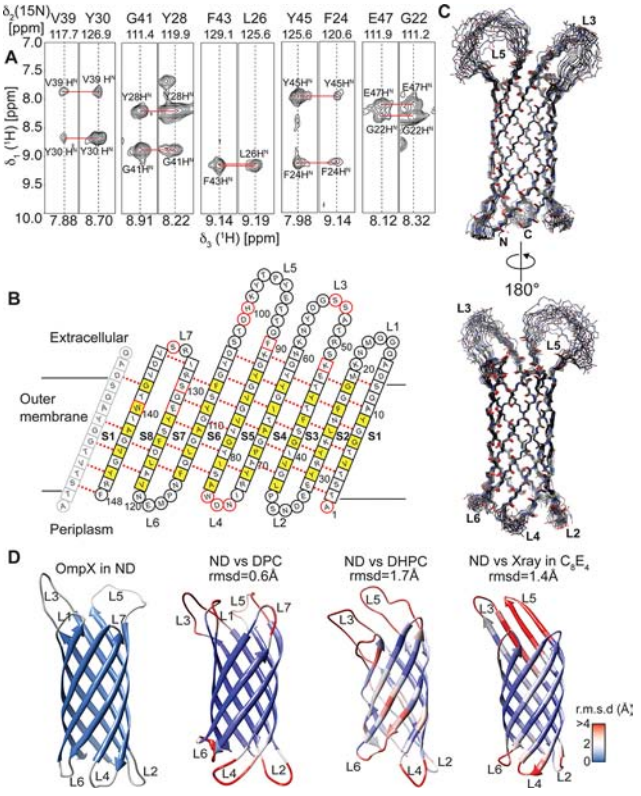

Figure 6. Structure determination of OmpX in nanodiscs. (A) Example strips taken from a 3D-^{15}N-edited-[^{1}H,^{1}H]-NOESY experiment showing long-range inter-β-strand contacts used for structure calculation. (B) Topology plot of OmpX. Residues facing toward the lipid bilayer are shown in yellow, unassigned residues in red. Residues in β-sheets are represented by squares, whereas residues in loop regions are represented by circles. (C) The best-energy structural ensemble (20 structures) of OmpX in nanodiscs has an rmsd of 0.32 Å between residues in β-sheets. (D) Comparison of the OmpX structure in nanodiscs (ND) with the NMR structures of OmpX in the detergents dodecylphosphocholine (DPC) (determined here), dihexanoyl-glycero-phosphocholine (DHPC),[15] and the crystal structure in *n*-octyltetraoxyethylene (C_8E_4).[16] These structures are color-coded according to the rmsd values to individual residues of the nanodisc structure, as shown by the legend on the lower right. The rmsd to ordered residues of the NMR structure in nanodiscs is indicated above each structure.

S7C). A comparison of the different OmpX structures obtained here and from previous studies[15,16] shows that the biggest differences are present within the extracellular loops, (color-coding and rmsd values in Figure 6D). The central eight-stranded β-barrel is present in all of the structures, yet there are slight differences in the length and relative orientation of these strands among the displayed structures, highlighting the influence of the different membrane mimics on the protein conformation.

Dynamics of OmpX in Phospholipid Nanodiscs and DPC Micelles. In order to probe the dynamical properties of OmpX in phospholipid bilayers and detergent micelles, we acquired ^{15}N heteronuclear NOE experiments for both systems (Figure 7A,B). The obtained data show that the dynamics in the nanosecond to picosecond range of most regions in the protein are not affected by the membrane mimic, in particular in the β-sheet region. These differences are more pronounced for the loop regions, especially loops 2 and 3. Loop 2 shows no marked dynamics (high hetNOE) in DPC micelles, whereas in the bilayer environment this region appears to be more flexible. The same tendency holds true for the long loop 3. Noteworthy, the generalized order parameter S^2 of OmpX in DPC and in nanodiscs calculated from chemical shift data agrees very well with the profile of experimental heteronuclear NOE values (black and red lines in Figure 7A,B).

These data emphasize that, besides structural differences, alterations in the membrane-mimicking environment can affect dynamical properties of OmpX, which might be relevant in terms of its functional features. In order to validate the structural differences between OmpX in the crystal and in solution, we further performed 25 ns MD simulations using the OmpX crystal structure (PDB code: 1qj8[16]) and the solution structure in nanodiscs obtained here as starting models, respectively. As can be seen in Figure 7A, the magnitude of the root-mean-square fluctuation (rmsf) values of the Cα atoms in both simulations resembles the pattern of the heteronuclear NOE values of OmpX in nanodiscs. This finding corroborates the NMR NOE, chemical shift and dynamics data and indicates, in line with previous results,[26] that loops 3 and 5 in OmpX do not adopt a well-ordered secondary structure in solution.

DISCUSSION

In this study, we showed that a detailed solution NMR characterization of integral polytopic membrane proteins in nanodiscs is feasible. The herein introduced truncated MSPs that assemble into markedly smaller nanodiscs are an important step toward that goal. In addition, the use of highly deuterated protein and lipids and advanced NMR sampling methods[23,24,27] also contribute to high-quality NMR spectra that can be recorded in short experimental time. Deuteration of lipids appears to be beneficial in particular for experiments involving

dx.doi.org/10.1021/ja310901f | J. Am. Chem. Soc. 2013, 135, 1919−1925

Table 2. Structural Statistics of OmpX in Phospholipid Nanodiscs and DPC[a]

	OmpX in nanodiscs	OmpX in DPC
Structural Information		
HN−HN NOEs (interstrand contacts)	58	50
hydrogen bond restraints	67	65
dihedral angle restraints (TALOS[21])	291	275
backbone rmsd for β-sheets (Å)[b]	0.32 ± 0.16	0.30 ± 0.14
backbone rmsd for all residues (Å)	1.32 ± 0.31	1.72 ± 0.33
Ramachandran Map Analysis[c]		
most favored regions	93.4%	90.2%
additionally allowed regions	4.1%	9.0%
generously allowed regions	1.6%	0.8%
disallowed regions	0.8%	0.0%
Deviations from Restraints and Idealized Geometry		
distance restraints (Å)	0.039 ± 0.001	0.044 ± 0.0008
dihedral angle restraints (deg)	0.127 ± 0.007	0.236 ± 0.01
bonds (Å)	0.0021 ± 0.00006	0.0023 ± 0.00008
angles (deg)	0.61 ± 0.01	0.65 ± 0.01
impropers (deg)	1.52 ± 0.07	2.35 ± 0.06

[a]Analysis of the 20 lowest-energy structures. [b]Order secondary structure elements were used for structural superimposition: 3−14, 20−30, 38−48, 60−71, 78−90, 104−115, 122−132, 135−147; rmsd values are calculated relative to a nonminimized average structure of each ensemble. [c]Ramachandran analysis with PROCHECK-NMR[25] was performed on the lowest-energy structure.

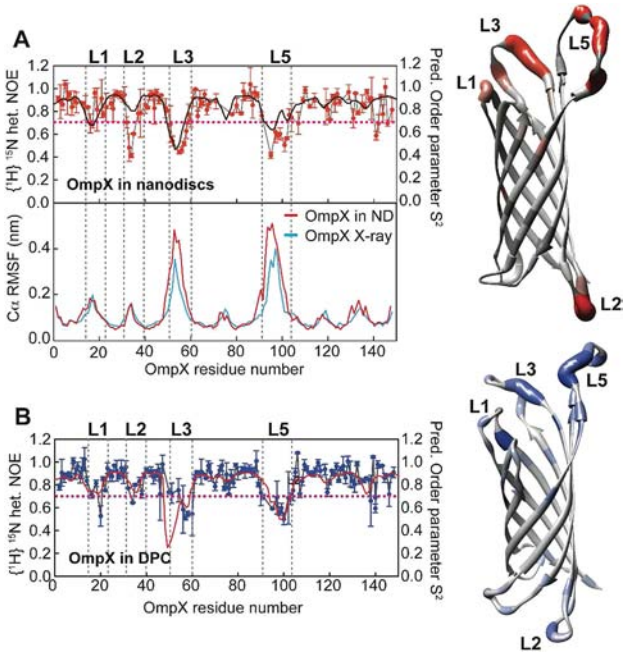

Figure 7. Dynamics of OmpX in nanodiscs and in DPC. (A) Upper left: {^{1}H}−^{15}N-heteronuclear NOE for OmpX in nanodiscs (red symbols) overlaid by the predicted squared order parameter S^2 (black line). Right: Heteronuclear NOE values mapped onto the structure of OmpX (from gray to red). Lower left: Molecular dynamics simulations of OmpX in a DMPC phospholipid bilayer using the NMR structure obtained here (red line) or the previous X-ray structure (blue line)[16] as starting conformations. The root-mean-square fluctuations (rmsf) of amino acid residues in OmpX are shown. Both simulations were run for 25 ns duration at 45 °C. Of note, even the well-ordered X-ray structure exhibits large fluctuations in the external long loop regions. (B) {^{1}H}-^{15}N-heteronuclear NOE for OmpX in DPC (blue symbols) overlaid by the predicted squared order parameter S^2 (red line) based on chemical shift data. Right: Heteronuclear NOE values mapped onto the structure of OmpX in DPC (from gray to blue). Except at loop 2, these values are almost identical to the hetNOE obtained in nanodiscs. The dotted line at a hetNOE value of 0.7 represents the cutoff for coloring of residues in the structure.

side-chain coherence-transfer steps like the 3D-HNCACB. We show that smaller nanodiscs can be constructed and adapted to the size of the target protein of interest. The smallest nanodisc produced here harbors only around 10 lipids per MSP molecule (20 per nanodisc) and might be suited for single transmembrane spanning helices and membrane-anchored soluble proteins, yet the lower stability of this smallest nanodisc might restrict its use to short-term experiments. However, the very stable ΔH4 and ΔH5MSPD1 variants are large enough to accommodate membrane proteins up to ∼30 kDa in molecular weight while still offering sufficiently improved spectral quality required for structural studies, as shown here with the 148-residue-protein OmpX and the 22 kDa seven-transmembrane α-helical protein bR. The inherent dynamics of the lipids in the smaller ΔH5 nanodisc as compared to the wild-type nanodisc does not seem to be restricted, as shown by proton relaxation experiments of the lipid resonances (Figure S5). For larger membrane proteins or membrane protein complexes, the use of the wild-type MSP might be required solely because of size constraints imposed by the chosen membrane protein.

While so far high-resolution NMR structures of membrane proteins could be obtained in detergent micelles or bicelles that facilitate structural work due to their small size, the presence of detergents may be unfavorable for stability, alter the interaction properties with partner proteins, and/or distort the native protein structure. Here, we report a NMR-derived solution structure of a polytopic integral membrane protein in detergent-free phospholipid nanodiscs, which we believe has not been achieved before. The obtained structure of OmpX in nanodiscs shows the same overall fold and topology for the transmembrane part as previously determined NMR[15] and X-ray structures.[16] However, there are pronounced local differences to the crystal structure determined in *n*-octyltetraoxyethylene and NMR structures determined in micelles. The X-ray structure differs most prominently at the extracellular extensions of the β-sheet. Presumably these extracellular segments are immobilized by crystal contacts and the cryogenic temperature used during data collection. In nanodiscs in solution, these external β-sheet regions do not form a regular structure as shown here by chemical shifts, NOE, NMR dynamics data, and MD simulations. This is consistent with previous solution NMR[15] and MD[26] data. A comparison with this previous NMR solution structure solved in DHPC micelles identifies differences in the arrangement and lengths of the β-strands, which might be caused by the use of different structure calculation software and/or the choice of detergent. To clarify the role of the membrane mimetic on protein structure and dynamics, we pursued backbone resonance assignments and a structure determination of OmpX in a different detergent (DPC vs DHPC) but using the same buffer as for nanodiscs. We calculated a structural ensemble using the same approach as demonstrated for the nanodisc system (Figures S6 and S7, Table 2). The resulting structure in DPC micelles is comprised of a well-defined β-barrel and shows an overall fold that is very similar to the structure determined in DHPC micelles.

However, compared to the nanodisc structure, on average each strand is up to two residues shorter (Figure 6D, Figure S7), which might be due to the slightly denaturing effect of the detergent at the water boundary and differences in hydrophobic coverage. In addition to these structural differences, dynamics in the nanosecond to picosecond time scale as measured by ^{15}N-heteronuclear NOE experiments reveal differences between OmpX in nanodiscs and in DPC micelles, mainly in the loop regions at the surface of the membrane mimetic. Our data hence indicate that the membrane mimetic can have a considerable impact on the conformational space of the embedded protein.

CONCLUSIONS

We present here the first example of a membrane protein structure solved in phospholipid nanodiscs. The use of the herein introduced smaller nanodiscs was a critical step in this process and enabled a detailed NMR spectroscopic characterization of OmpX in a phospholipid bilayer system. We expect that the use of a native-like membrane environment might be even more important for marginally stable membrane proteins, which so far eluded structural studies due to limited stability in detergent micelles. Phospholipid nanodiscs may turn out to be an ideal choice for maintaining longer-term stability for structural studies, preserving a particular membrane protein in its functional form, and enabling binding studies in a detergent-free environment. With the introduction of the smaller MSP variants described here, solution NMR spectroscopy shows great promise to address important functional and structural questions of membrane proteins in their native lipid bilayer environment.

ASSOCIATED CONTENT

Supporting Information

Experimental details, SEC and EM data, as well as NMR data on OmpX in DPC. This material is available free of charge via the Internet at http://pubs.acs.org. The NMR backbone assignments and structural coordinates of OmpX in MSP1D1ΔH5 nanodiscs and in DPC micelles were deposited at the BMRB (accession codes 18796 and 18797) and RCSB (accession codes 2m06 and 2m07) databanks.

AUTHOR INFORMATION

Corresponding Author

gerhard_wagner@hms.harvard.edu

Author Contributions

‡M.E. and T.R. contributed equally.

Notes

The authors declare no competing financial interest.

ACKNOWLEDGMENTS

This work was supported by NIH grants GM047467 and GM094608 (to G.W.). F.H. was supported by EMBO and Human Frontier Science Program long-term fellowships. The molecular electron microscopy facility at Harvard Medical School is maintained with funds from NIH grant PO1 GM62580 (to Stephen C. Harrison). Maintenance and operation of the high-field NMR instruments used were supported by NIH grant P41-EB002026 (to Robert Griffin). FB Reagents (Cambridge, MA) is gratefully acknowledged for providing deuterated lipids (d_{54}-DMPC/d_{54}-DMPG). We thank Melissa Chambers and Tom Walz (Harvard Medical School) for help with electron microscopy and Scott Robson and Sven Hyberts (Harvard Medical School) for help with non-uniform sampling NMR setup. The simulations in this paper were run on the Orchestra cluster supported by the Harvard Medical School Research Information Technology Group.

REFERENCES

(1) Linke, D. *Methods Enzymol.* **2009**, *463*, 603.
(2) Lee, A. G. *Biochim. Biophys. Acta* **2003**, *1612*, 1.
(3) Seddon, A. M.; Curnow, P.; Booth, P. J. *Biochim. Biophys. Acta* **2004**, *1666*, 105.
(4) Frauenfeld, J.; Gumbart, J.; Sluis, E. O.; Funes, S.; Gartmann, M.; Beatrix, B.; Mielke, T.; Berninghausen, O.; Becker, T.; Schulten, K.; Beckmann, R. *Nat. Struct. Mol. Biol.* **2011**, *18*, 614.
(5) Denisov, I. G.; Grinkova, Y. V.; Lazarides, A. A.; Sligar, S. G. *J. Am. Chem. Soc.* **2004**, *126*, 3477.
(6) Judge, P. J.; Watts, A. *Curr. Opin. Chem. Biol.* **2011**, *15*, 690.
(7) Ritchie, T. K.; Grinkova, Y. V.; Bayburt, T. H.; Denisov, I. G.; Zolnerciks, J. K.; Atkins, W. M.; Sligar, S. G. *Methods Enzymol.* **2009**, *464*, 211.
(8) Nath, A.; Atkins, W. M.; Sligar, S. G. *Biochemistry* **2007**, *46*, 2059.
(9) Krieger, M.; Brown, M. S.; Faust, J. R.; Goldstein, J. L. *J. Biol. Chem.* **1978**, *253*, 4093.
(10) Fang, Y.; Gursky, O.; Atkinson, D. *Biochemistry* **2003**, *42*, 13260.
(11) Raschle, T.; Hiller, S.; Yu, T. Y.; Rice, A. J.; Walz, T.; Wagner, G. *J. Am. Chem. Soc.* **2009**, *131*, 17777.
(12) Yu, T. Y.; Raschle, T.; Hiller, S.; Wagner, G. *Biochim. Biophys. Acta* **2012**, *1818*, 1562.
(13) Gluck, J. M.; Wittlich, M.; Feuerstein, S.; Hoffmann, S.; Willbold, D.; Koenig, B. W. *J. Am. Chem. Soc.* **2009**, *131*, 12060.
(14) Shenkarev, Z. O.; Lyukmanova, E. N.; Paramonov, A. S.; Shingarova, L. N.; Chupin, V. V.; Kirpichnikov, M. P.; Blommers, M. J.; Arseniev, A. S. *J. Am. Chem. Soc.* **2010**, *132*, 5628.
(15) Fernandez, C.; Adeishvili, K.; Wuthrich, K. *Proc. Natl. Acad. Sci. U.S.A.* **2001**, *98*, 2358.
(16) Vogt, J.; Schulz, G. E. *Structure* **1999**, *7*, 1301.
(17) Borhani, D. W.; Rogers, D. P.; Engler, J. A.; Brouillette, C. G. *Proc. Natl. Acad. Sci. U.S.A.* **1997**, *94*, 12291.
(18) Fischer, N. O.; Blanchette, C. D.; Segelke, B. W.; Corzett, M.; Chromy, B. A.; Kuhn, E. A.; Bench, G.; Hoeprich, P. D. *PLoS One* **2010**, *5*, e11643.
(19) Schwarz, D.; Junge, F.; Durst, F.; Frolich, N.; Schneider, B.; Reckel, S.; Sobhanifar, S.; Dotsch, V.; Bernhard, F. *Nat. Protoc.* **2007**, *2*, 2945.
(20) Lee, D.; Hilty, C.; Wider, G.; Wuthrich, K. *J. Magn. Reson.* **2006**, *178*, 72.
(21) Shen, Y.; Delaglio, F.; Cornilescu, G.; Bax, A. *J. Biomol. NMR* **2009**, *44*, 213.
(22) Salzmann, M.; Pervushin, K.; Wider, G.; Senn, H.; Wuthrich, K. *Proc. Natl. Acad. Sci. U.S.A.* **1998**, *95*, 13585.
(23) Hyberts, S. G.; Takeuchi, K.; Wagner, G. *J. Am. Chem. Soc.* **2010**, *132*, 2145.
(24) Hyberts, S. G.; Milbradt, A. G.; Wagner, A. B.; Arthanari, H.; Wagner, G. *J. Biomol. NMR* **2012**, *52*, 315.
(25) Laskowski, R. A.; Rullmannn, J. A.; MacArthur, M. W.; Kaptein, R.; Thornton, J. M. *J. Biomol. NMR* **1996**, *8*, 477.
(26) Choutko, A.; Glattli, A.; Fernandez, C.; Hilty, C.; Wuthrich, K.; van Gunsteren, W. F. *Eur. Biophys. J.* **2011**, *40*, 39.
(27) Hyberts, S. G.; Arthanari, H.; Wagner, G. *Top. Curr. Chem.* **2012**, *316*, 125.